

## AlGaN/GaN polarization-doped field-effect transistor for microwave power applications

Siddharth Rajan,<sup>a)</sup> Huili Xing, Steve DenBaars, and Umesh K. Mishra  
*Department of Electrical and Computer Engineering and Materials Department, University of California, Santa Barbara, California 93106*

Debdeep Jena  
*Department of Electrical Engineering, University of Notre Dame, Notre Dame, Indiana 46556*

(Received 30 October 2003; accepted 8 January 2004)

We discuss an AlGaN/GaN metal–semiconductor field-effect transistor (MESFET) structure grown without any impurity doping in the channel. A high-mobility polarization-induced bulk channel charge was created by grading the channel region linearly from GaN to Al<sub>0.3</sub>Ga<sub>0.7</sub>N over 1000 Å. This polarization-doped FET (PoIFET) was fabricated and tested under dc and rf conditions. Current density of 850 mA/mm and transconductance of 93 mS/mm was observed under dc conditions. The 0.7 μm gate length devices had a cutoff frequency,  $f_T=19$  GHz, and maximum oscillation frequency,  $f_{max}=46$  GHz. We demonstrate that the PoIFETs perform better than comparable MESFETs with impurity-doped channels, and are suitable for high power microwave applications. An important advantage of these devices over AlGaN/GaN high electron mobility transistors is that the transconductance versus gate voltage profile can be tailored by compositional grading for better large-signal linearity. © 2004 American Institute of Physics. [DOI: 10.1063/1.1652254]

In recent years, III–V nitrides have emerged as important materials for high-power microwave electronic applications.<sup>1,2</sup> In the most successful nitride electronic devices, high electron mobility transistors (HEMTs), the spontaneous and piezoelectric polarization fields in AlGaN and GaN are used to create a two-dimensional electron gas (2DEG) with high carrier concentration. These devices have yielded excellent power and efficiency performance at microwave frequencies.

In addition to high power and efficiency, devices for many wireless applications are also required to have high linearity at microwave frequencies. Design of such linear devices for large-signal operation needs tailoring of the transconductance ( $g_m$ ) profile over the input gate voltage ( $V_g$ ) range. However, the structure of AlGaN/GaN HEMT-like devices does not lend itself to easy modification of the  $g_m-V_{gs}$  profile. It has been shown that the  $g_m-V_{gs}$  curve of metal–semiconductor field-effect transistors (MESFETs) can be tailored by designing the channel doping profile.<sup>3–5</sup> GaN MESFETs therefore remain attractive for high-linearity microwave power applications. However, the device designer is constrained in his choice of channel charge due to gate leakage, breakdown and impurity scattering limited mobility.

In AlGaN/GaN HEMTs, a fixed sheet charge is formed at the heterointerface due to the piezoelectric polarization in the strained AlGaN and the discontinuity in the spontaneous polarization at the interface. To screen the net positive charge at the AlGaN/GaN junction, a 2DEG forms. Jena *et al.*<sup>11</sup> have shown that the same effect can also be used to create a bulk three-dimensional electron slab. This is achieved by grading from GaN to AlGaN, thus spreading the polarization-induced charge over the graded region. The

polarization-induced carrier density,  $\rho_\pi$ , is given by the equation  $\rho_\pi=\nabla\cdot\mathbf{P}$ ; here  $\mathbf{P}$  is the total polarization in the material. Since the AlGaN composition and polarization are shown to be approximated well by Vegard's law, any desired channel charge profile can be obtained by choosing the appropriate grading scheme. This can be used to tailor the  $g_m-V_{gs}$  profile of a polarization-doped field-effect transistor (PoIFET). This is analogous to impurity doped MESFETs, where the  $g_m-V_{gs}$  profile is modified by the dopant profile design.

A PoIFET is expected to have many advantages over conventional MESFETs. Since the PoIFET channel is polarization doped, there is no ionized impurity scattering, and the electron mobility is much higher than in impurity-doped MESFETs. This property can be used to make highly conductive channels and access regions in devices. Gate leakage is an important problem in MESFETs since the Schottky barrier to GaN is low. This is improved in the PoIFET because the channel is graded from GaN to AlGaN, leading to a higher effective barrier height. AlGaN has a higher breakdown field than GaN, which permits the use of higher channel charge concentrations. Therefore, the PoIFET structure permits a higher channel charge than a conventional MESFET, but still allows the designer to modify the channel carrier concentration profile.

Impurity-doped MESFETs cannot operate at lower temperatures due to the freeze out of carriers. Since the mobile carriers in the PoIFET are *electrostatically* induced by the fixed polarization charge, there is no freeze out at lower temperatures. As in a HEMT, the performance of the PoIFET improves at lower temperatures since phonon scattering is reduced, and the mobility is higher.<sup>11</sup>

For comparison, two samples, a conventional impurity-doped MESFET and a polarization-doped FET, or PoIFET, were studied (Fig. 1). The samples were grown by metalor-

<sup>a)</sup>Electronic mail: srajan@ece.ucsb.edu

5 nm UID GaN cap	5 nm UID GaN cap
100 nm GaN:Si $10^{18} \text{ cm}^{-3}$	100 nm 0-30% AlGaN $1.6 \times 10^{18} \text{ cm}^{-3}$
1.7 $\mu\text{m}$ GaN:UID	1.7 $\mu\text{m}$ GaN:UID
0.7 $\mu\text{m}$ Fe-doped GaN	0.7 $\mu\text{m}$ Fe-doped GaN
50 nm AlN	50 nm AlN
Sapphire	Sapphire
(a)	(b)

FIG. 1. Epitaxial structure of the (a) MESFET and (b) PoIFET.

ganic chemical vapor deposition (MOCVD) on sapphire substrates. Both devices have the same buffer layer, which consists of 0.7  $\mu\text{m}$  Fe-doped GaN, followed by 50 nm AlN and 1.7  $\mu\text{m}$  unintentionally doped (UID) GaN. For the PoIFET, this was followed by a 100 nm channel consisting of GaN linearly graded to  $\text{Al}_{0.3}\text{Ga}_{0.7}\text{N}$ . In the case of the MESFET, the channel consists of 100 nm of GaN:Si doped at  $10^{18} \text{ cm}^{-3}$ . Both devices had a 5 nm UID GaN cap.

The calculated band diagram of the PoIFET structure at zero bias is shown in Fig. 2(a). The band diagram was calculated using a self-consistent one-dimensional Schrödinger–Poisson solver with built-in polarization fields.<sup>12</sup> A Schottky barrier height of 0.9 eV at the top surface of the structure was assumed. The carrier profile from CV measurements agrees well with the simulated profile, as shown in Fig. 2(b). An average charge of  $1.6 \times 10^{18} \text{ cm}^{-3}$  was measured for a linear grade up to 30% AlGaN over 100 nm. The MESFET sample was found to have a carrier concentration of  $10^{18} \text{ cm}^{-3}$  in the channel. Hall mobilities were measured to be  $826 \text{ cm}^2/\text{Vs}$  for the PoIFET sample and  $284 \text{ cm}^2/\text{Vs}$  for the MESFET. As expected, the mobility in the polarization-doped sample is higher than the impurity-doped MESFET sample.

Field-effect transistors were fabricated on both samples. Ohmic contacts were made by evaporating Ti/Al/Ni/Au and annealing at  $870^\circ\text{C}$ . Mesa isolation was performed using  $\text{Cl}_2$  reactive ion etching. Ni/Au contacts were evaporated for the gate metal, and the surface was passivated with silicon nitride to reduce high-frequency dispersion. The devices fabri-

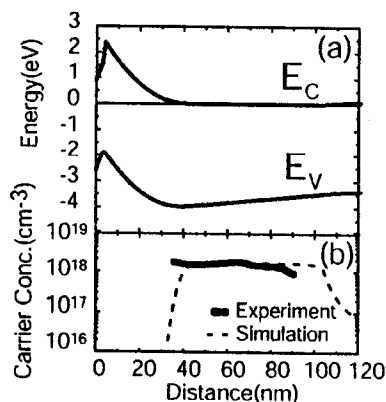


FIG. 2. (a) Zero bias band diagram of the PoIFET assuming a 0.9 eV Schottky barrier for the metal–GaN junction. (b) Carrier concentration profiles from experiment (CV measurements) and simulations. This structure was simulated using BandEng (Ref. 12).

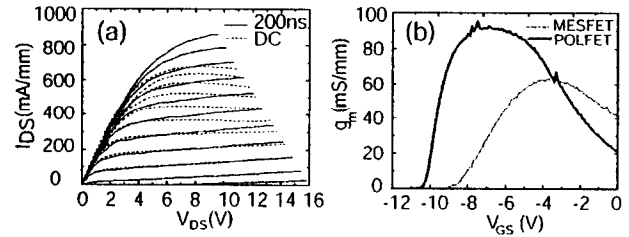


FIG. 3. (a) Dc and 200 ns pulsed  $I-V$  characteristics of the PoIFET (after passivation). The device dimensions are  $L_g = 0.7 \mu\text{m}$  and  $W = 150 \mu\text{m}$ . The gate was biased at  $-10 \text{ V}$  and 200 ns pulses were applied. The topmost curves represent  $V_G = 0 \text{ V}$ . (b) Transconductance for the PoIFET and MESFET with  $L_g = 0.7 \mu\text{m}$  and  $W = 150 \mu\text{m}$ . The drain bias was 10 V.

cated were  $150 \mu\text{m}$  wide, with gate length of  $0.7 \mu\text{m}$  and source–drain spacing of  $3.4 \mu\text{m}$ .

Dc and 200 ns pulsed  $I-V$  plots for the PoIFET are shown in Fig. 3(a). The pulsed drain current at zero gate bias for the PoIFET was  $850 \text{ mA/mm}$  and the pinch-off voltage was  $-10 \text{ V}$ . The dc currents are lower than the pulsed values at higher current levels due to self-heating in the sample. In comparison, the MESFET had a lower current ( $600 \text{ mA/mm}$ ) and were pinched off at  $-8 \text{ V}$  gate bias, due to lower charge. The knee voltage for the PoIFET was 5 V, which is lower than the MESFET value of 7 V. This is because of the lower sheet resistance in the PoIFET. The MESFET was also found to have high gate leakage and a low breakdown due to the high level of doping in the channel. The PoIFET, on the other hand, had less gate leakage, and higher breakdown voltage in spite of the higher channel charge.

The measured variation of transconductance,  $g_m$ , with the gate bias,  $V_{GS}$ , at drain voltage of 10 V is shown in Fig. 3(b). The peak transconductance for the PoIFET,  $93 \text{ mS/mm}$ , is a very high reported value for a GaN MESFET device. The dip in transconductance at higher drain voltages and currents is due to the self-heating in the sample.

High frequency small-signal characterization of the devices from 50 MHz to 40 GHz was carried out, and the current gain ( $h_{21}$ ) and the unilateral power gain (GTU) were calculated from the measured  $s$  parameters of the device. Figure 4 shows  $h_{21}$  and GTU as a function of the input signal frequency. The measured  $f_T$  and  $f_{\text{max}}$  values were 18.6 and 46 GHz, respectively. The device was biased at  $V_{DS} = 15 \text{ V}$  and  $I_{DS} = 100 \text{ mA/mm}$ . In Table I, the  $f_T$  and  $f_{\text{max}}$  values of the PoIFET are compared with earlier MESFET and junction field-effect transistor results. The PoIFET outperforms all past MESFETs due to its higher mobility and charge. Also,

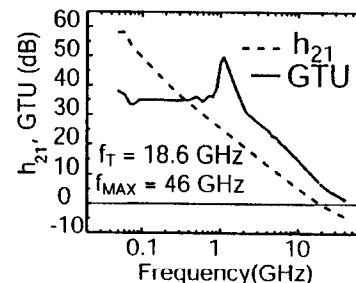


FIG. 4. Unilateral power gain (GTU) and current gain ( $h_{21}$ ) from small-signal measurements of the PoIFET.  $f_T$  and  $f_{\text{max}}$  were 18.6 and 46 GHz, respectively. The device was biased at  $V_{DS} = 15 \text{ V}$  and  $I_{DS} = 100 \text{ mA/mm}$ .

TABLE I. Comparison between PolFET and previous field-effect transistors (NR: not reported, JFET: junction field-effect transistors).

Author(s)	Year	Device	$g_m$	$L_g$	$f_t$	$f_{max}$	Power
This work	2003	PolFET	93 mS/mm	0.7 $\mu\text{m}$	18.6 GHz	44 GHz	NR
Gaska <i>et al.</i> (Ref. 8)	2002	MESFET	NR	1.5 $\mu\text{m}$	6 GHz	12 GHz	0.6 W/mm at 2 GHz
Jiménez <i>et al.</i> (Ref. 6)	2001	JFET	67 mS/mm	0.7 $\mu\text{m}$	NR	NR	NR
Gaquiére <i>et al.</i> (Ref. 7)	2000	MESFET	NR	0.3 $\mu\text{m}$	11 GHz	NR	2.2 W/mm at 2 GHz
Lee <i>et al.</i> (Ref. 10)	2000	MESFET	36 mS/mm	0.25 $\mu\text{m}$	26 GHz	54 GHz	NR
Binari <i>et al.</i> (Ref. 9)	1994	MESFET	20 mS/mm	0.7 $\mu\text{m}$	8 GHz	17 GHz	NR

the PolFET performs as well as a typical AlGaN/GaN HEMT with similar gate length.

In summary, polarization-doped GaN FETs were grown and fabricated on sapphire substrates. They were found to have good dc and small-signal performance with  $g_m = 93$  mS/mm,  $f_t = 19$  GHz, and  $f_{max} = 46$  GHz. PolFETs therefore look very promising for high-frequency, high-power applications. An important advantage of these devices over HEMTs is that they allow optimization of the  $g_m - V_{gs}$  profile thereby improving linearity. Design and measurement of PolFETs for power and linearity performance are currently underway. As an added advantage, PolFETs are expected to perform well at lower temperatures where impurity-doped MESFETs fail due to carrier freeze out. Temperature-dependent measurements to study the enhanced performance of these devices at lower temperatures are being carried out. Finally, we note that PolFET-like structures can be realized in any material system that possess sufficiently high spontaneous or piezoelectric polarization. Oxides and other II-VI semiconductors with suitable properties can therefore be used for devices that utilize polarization doping.

The authors thank Robert Coffie, Alessandro Chini, and Likun Shen for helpful discussions. Funding from CNSI,

AFOSR (contract monitor: Gerald Witt) and ONR POLARIS MURI (contract monitor: Colin Wood) is gratefully acknowledged.

<sup>1</sup>U. K. Mishra, P. Parikh, and Y. F. Wu, Proc. IEEE **90**, 1022 (2002).

<sup>2</sup>L. F. Eastman and U. K. Mishra, IEEE Spectrum **39**, 28 (2002).

<sup>3</sup>R. E. Williams and D. W. Shaw, IEEE Trans. Electron Devices **ED-25**, 600 (1978).

<sup>4</sup>R. Pucel, Electron. Lett. **14**, 204 (1978).

<sup>5</sup>J. A. Higgins and R. L. Kuvas, IEEE Trans. Microwave Theory Tech. **MTT-28**, 9 (1980).

<sup>6</sup>A. Jiménez, D. Buttari, D. Jena, R. Coffie, S. J. Heikman, N. Zhang, L. Shen, E. Calleja, E. Muñoz, J. S. Speck, and U. K. Mishra, IEEE Electron Device Lett. **23**, 306 (2002).

<sup>7</sup>C. Gaquiére, S. Trassaert, B. Boudart, and Y. Crosnier, IEEE Microw. Guid. Wave Lett. **10**, 19 (2000).

<sup>8</sup>R. Gaska, M. Asif Khan, X. Hu, G. Simin, J. Yang, J. Deng, S. Rumyantsev, and M. S. Shur, Appl. Phys. Lett. **78**, 769 (2001).

<sup>9</sup>S. C. Binari, L. B. Rowland, W. Kuppa, G. Kelner, K. Doverspike, and D. K. Gaskill, Electron. Lett. **30**, 1248 (1994).

<sup>10</sup>C. Lee, W. Lu, E. Piner, and I. Adesida, *58th Device Research Conference*, 19–21 June 2000, Denver, CO (DRC Digest, 2000), p. 41.

<sup>11</sup>D. Jena, S. Heikman, D. Green, D. Buttari, R. Coffie, H. Xing, S. Keller, S. DenBaars, J. S. Speck, and U. K. Mishra, Appl. Phys. Lett. **81**, 4395 (2002).

<sup>12</sup>M. Grundmann, BandEng Alpha Version (2003); <http://my.ece.ucsb.edu/mgrundmann/bandeng.htm>.